J Nanostruct 16(1): 421-434, Winter 2026

RESEARCH PAPER

Green Synthesis of Chitosan-Coated Selenium Nanoparticles Using Pomegranate Peel Extract: Antifungal Activity Against Candida spp. and Cytotoxicity on MCF7 Cells

Zahraa Mohammed Ahmed, Mais Emad Ahmed *

Department of Biology, College of Science, University of Baghdad, Jadriya, Baghdad, Iraq

ARTICLE INFO

Article History:
Received 11 August 2025
Accepted 05 December 2025
Published 01 January 2026

Keywords:
CCS NP
Green Synthesis
MCF7 Cells
SEM
XRD

ABSTRACT

Rapid industrialization and growing economic activity have contributed to an increase in environmental waste, driving the demand for green and sustainable technologies. This study describes the eco-friendly biosynthesis of bimetallic selenium nanoparticles (SeNPs) using pomegranate peel extract (PPE), followed by stabilization with nano-chitosan to form a nanocomposite (CS/SeNPs). The synthesized nanocomposite was characterized using FTIR, XRD, UV–Vis spectroscopy, SEM, and EDX, confirming the presence of uniformly distributed, spherical nanoparticles. Antifungal activity was tested against Candida albicans, Candida guilliermondii, and Candida ferric. The CS/SeNPs nanocomposite exhibited significantly greater antifungal activity than SeNPs alone, with notable inhibition zones ($p < 0.05$). The Minimum Inhibitory Concentration (MIC) of the SNPs ranged from 64 to 1000 µg/ml. In vitro cytotoxicity testing, performed using the MTT assay, against the human breast cancer cell line MCF-7, demonstrated dose-dependent anticancer activity. The CS/SeNPs nanocomposite showed a half-maximal inhibitory concentration (IC50) exceeding 11 µg/ml, indicating low cytotoxicity and potential biomedical safety. The cytotoxic effects were attributed to apoptosis induction and oxidative stress mechanisms. Overall, the results highlight the dual therapeutic potential of CS/SeNPs as both an antifungal agent and a selective anticancer nanomaterial. This study suggests that green-synthesized CS/SeNPs may serve as a promising candidate in the development of novel therapies targeting fungal infections and multidrug-resistant cancers. Further in vivo studies and pharmacokinetic evaluations are needed to support clinical translation. Keywords: Na_2SeO_3, pomegranate peel, X-ray diffraction (XRD), Candida spp, cell line MCF7.

How to cite this article
Ahmed Z., Ahmed M. Green Synthesis of Chitosan-Coated Selenium Nanoparticles Using Pomegranate Peel Extract: Antifungal Activity Against Candida spp. and Cytotoxicity on MCF7 Cells. J Nanostruct, 2026; 16(1):421-434. DOI: 10.22052/JNS.2026.01.038

INTRODUCTION

Nanomaterials are typically synthesized using two main approaches: the top-down and bottom-up methods. The top-down approach involves breaking down bulk materials into nanoscale structures using physical techniques such as laser ablation, vapor deposition, and ball milling. While biological methods utilize plant extracts,

* *Corresponding Author Email: mais.emad@sc.uobaghdad.edu.iq*

fungi, bacteria, and other natural agents for green synthesis [1]. In recent years, chemical and physical synthesis methods have been used less frequently due to their associated environmental and health hazards. In contrast, biological synthesis has emerged as a more sustainable alternative, offering advantages such as cost-effectiveness, safety, simplicity, and environmental friendliness. The green synthesis approach emphasizes minimizing the use of hazardous chemicals, particularly toxic substances. Moreover, it aligns with the twelve principles of green chemistry, which advocate for the development of safer, less harmful products and processes [2]. In the green synthesis of nanomaterials, naturally occurring organic compounds in plants such as terpenoids, alkaloids, and various polyphenols—serve as both reducing and capping agents. This eco-friendly approach utilizes different parts of plants, fungi, and microbes for nanoparticle synthesis. The adsorption of plant-derived biomolecules onto the surface of the nanoparticles can reduce their potential toxicity [3]. Selenium is an essential trace micronutrient required by most living organisms. In humans, insufficient selenium levels can negatively affect immune function. Selenium is a key component of various functional proteins, including selenoproteins, which play crucial roles in immune system regulation and exhibit notable anticancer properties [4]. The biogenic synthesis of selenium nanoparticles (SeNPs) has gained considerable attention in recent years due to their distinctive physical and chemical properties. During this green synthesis process, selenium in the +4 oxidation state (Se^{4+}) is reduced to elemental selenium (Se^{o}). Selenium nanoparticles produced via biological methods exhibit notable biological activities [5]. The peel and extract of pomegranates (Punica granatum L.) and their applications as food additives, functional foods, or physiologically active ingredients in nutraceutical compositions [6]. The nutritional composition of pomegranate peel is noteworthy, as it contains significant amounts of dietary fiber, vitamins (particularly vitamin C), and minerals like potassium. The components of pomegranate peel and extract contribute to their overall nutritional value, making them a suitable candidate for inclusion in functional foods and supplements [7]. Chitosan is a renewable natural polymer obtained

Fig. 1. Preparation CS/ SeNPs.

through the deacetylation of chitin. It contains several reactive functional groups, such as hydroxyl (-OH) and amino (-NH_2) groups. Due to its hydrophilic nature, biocompatibility, non-toxicity, biodegradability, and cost-effectiveness, chitosan is widely recognized and utilized [8]. A systematic approach was employed to synthesize and evaluate green-synthesized selenium nanoparticles (SeNPs) coated with nano-chitosan, forming a nanocomposite (NCS-Se NPs). In this formulation, chitosan nanoparticles not only stabilize the SeNPs but also contribute inherent antifungal properties. The study assessed the antifungal activity of individual components—bulk materials and nanoparticles compared to the complete nanocomposite. Additionally, the synergistic effects and minimum inhibitory concentration (MIC) of NCS-Se NPs were determined to evaluate their potential as an effective biocontrol agent [9] Although in vivo validation is still lacking, previous studies have suggested that selenium nanoparticles (SeNPs) stabilized with pure chitosan can exhibit anticancer activity. Additionally, the molecular weight of chitosan has been shown to influence both the release profile of SeNPs and potential changes in their valence state in vitro. The current investigation aimed to explore the ability of known antifungal and anticancer agents to stabilize selenium nanoparticles within chitosan-based nanocarriers, thereby enhancing their therapeutic potential and stability.

MATERIALS AND METHODS

Pomegranate Peel Extract (PPE)

Fruit peels from organically grown pomegranates (Punica granatum L.) were manually obtained after the fruits were washed with double-distilled water (DW) and allowed to air-dry for 62 hours at 44 ± 2 °C. After being mechanically ground into a powder (100 g, approximately 60 mesh size), the dried peels were extracted employing 1 L of 70% diluted ethanol, stirred at 110×g for 65 hours at room temperature (RT; 25 ± 2 °C), and filtered to get rid of any remaining plant debris. To obtain a 10% concentration, the P. granatum peel extract (PPE) was redissolved in DW after being vacuum-dried at 41 °C. [10].

Green synthesis of PPE- Selenium nanoparticles (SeNPs)

An aqueous solution of sodium selenite "Na_2SeO_3" (10 mM) has been made in DW. A Na_2SeO_3 solution (10 mM) and 10 ml of PPE (1%, w/v) were subsequently combined and stirred at 610 × g for 55 minutes at room temperature. The brownish-orange color of the fluid indicated the PPE biosynthesis of SeNPs. PPE/SeNPs matrix was precipitated from the solution by centrifugation at 11.600 ×g for 37 minutes. Parts of the PPE/SeNPs matrix were then centrifuged to produce plain SeNPs after being washed three times with DW and twice with ethanol. The PPE/SeNPs and ordinary SeNPs were then freeze-dried [11].

Chitosan loading Selenium nanoparticles CS/SeNPs

CS loading and preparation using PPE/SeNPs was taken from previously demonstrated experiments (Fig. 1) CS solution (2.5 wt%) was prepared in the 1% ascorbic acid. About 1.5mL of the synthesized SeNPs media was added to 5mL of the CS solution with stirring at room temperature till complete homogenization upheld PPE/ SeNPs in conjugation with the CT which was then centrifuged, washed with DW, and lyophilized [12].

Nanoparticles ultrastructure

Utilizing a 20 kV accelerating voltage, the SEM (scanning electron microscope) was used to screen for ultrastructure, including the topography and dispersion of particles. TEM imaging was utilized to further check the PPE-synthesised SeNPs' ultrastructure, particularly its shape, dispersion, and Ps.

Characterization of SeNPS

Fourier transform infrared spectroscopy (FTIR) (FTIR, Bruker Co., Ettlingen, Germany). SeNPs was performed by scanning the wavelength range of 400–4000 cm^{-1}. , energy dispersive X-ray (EDX), atomic force microscopy (AFM), ultraviolet-visible spectroscopy (UV-VIS) SeNPs was measured From 200 to 600 nm using a UV–Vis spectrophotometer (UV/Vis-1800,Shimadzu, Kyoto, Japan). , and X-ray diffraction (XRD) were used to investigate the shape and dimension of the Se NPs Powdered sample Sample Slurry/Smear Slide Mount for Small Sample Amounts. The images were taken with a scanning electron microscope (SEM) with a resolution of 500 nm (Hitachi s-3400N). Energy-dispersive X-ray analysis EDX analysis analysis can be used to identify the qualitative and quantitative state of elements that may be involved in the formation of nanoparticles. This examination was

conducted at University of Baghdad's College of Sciences Department of Chemistry labs served [13].

Determination of minimum Inhibition Concentration (MIC) of CS-SeNPs

The microdilution method was used to determine the minimum inhibitory concentrations (MICs) of CS-SeNPs against indicator strains, as was previously reported [14]. Every indicator strain was grown for an entire night in the appropriate medium. Using the proper culture medium chosen based on indicator fungi, we dissolved and diluted CS-SeNPs. The broth microdilution method was used to determine the minimum inhibitory concentration (MIC) of Chi-CuNPs against several pathogenic fungi. Different concentrations of Chi-CuNPs (1000, 500, 250, 125, and 62.5 µg/mL) were produced. Mueller-Hinton Agar was used to produce bacteria and Candida species to test CS-SeNPs. After that, the agar-well diffusion assay was used.

Antifungal susceptibility to the CS-SeNPs by agar diffusion test

The disc diffusion agar and MIC techniques were used to test for susceptibility. The Clinical and Laboratory Standards Institute (CLSI)-recommended broth microdilution reference method was used to test antifungal susceptibility in duplicate. Candida albicans, Candida krusei, and Candida glabrata are three common drug-resistant strains. were isolated and identified from the biology department of Baghdad University in Iraq. They were then cultivated on plates that contained Sabouraud dextrose agar media (Merck). The agar well diffusion method was used to examine the synthetic CS-Se-NPs efficacy against clinical isolates To produce confluent Fungal growth, sterile cotton-tipped swabs were used to inoculate Mueller-Hinton agar (MHA) plates with a pure fungal suspension from an overnight culture on nutritional agar medium at 37°C. Using a sterile borer, five wells spaced equally apart were positioned on the agar surface. Each well received

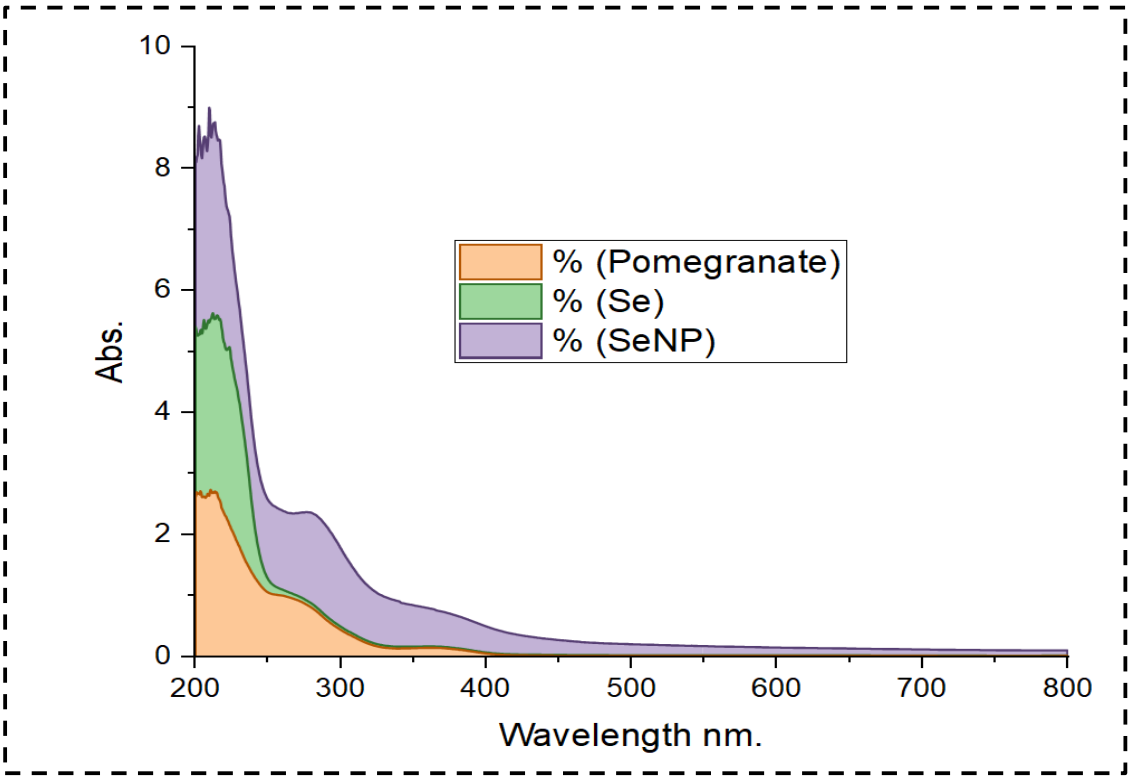

Fig. 2. UV—vis spectroscopy analysis a) pomegranate peel extract, b) Na_2SeO_3 c) Selenium nanoparticles.

80 µL of the tested NPs suspension in MHB (2000 µg/ml). All plates were refrigerated for 30 minutes to allow the NPs suspension to pre-diffuse into the MHA. A 24-hour aerobic incubation period at 37°C came next. Measured in triplicate throughout the investigation, the diameter of the clear zone that formed around NP-containing wells has been displayed as mean ± standard deviation (mean ± SD)[15].

Cytotoxicity assay

An in vitro 3-(4, 5-dimethylthiazol-2-yl)-2,5-diphenyltetrazolium bromide (MTT) test was used to evaluate the cytotoxic effects. To guarantee cell adherence, 7,000 cells were cultured overnight in each well of a 96-well plate. Subsequently, MCF7 cell lines were exposed to substances at increasing concentrations of CS-Cu NPs (6.25–100 µg/ml); three replicate wells were used for each treatment. Following a 24-hour incubation period, the medium was removed from the plate, and 20 µl of Shanghai Macklin Biochemical Co., Ltd.'s MTT solution (5 mg/ml) was added to each well. After that, the wells were incubated in the dark at 37˚C for three hours. The MTT was agitated for 10 minutes to dissolve the 50 µl of DMSO (Bio Basic Inc.) that had been added [16]. Absorbance at 490 nm was measured using a microplate reader From the raw absorbance data, the proportion of live cells was calculated using the following formula.

$$\text{Viability } \% = \frac{\text{A (test)} - \text{A (blank)}}{\text{A (control)} - \text{A (blank)}} \times 100$$

Where the absorbance is denoted by "A." GraphPad Prism software version 6 (Dotmatics) was used to create the dose-response curve, and the same curve was used to calculate the growth inhibitory concentration (IC50), which lowers viability by 50% [17].

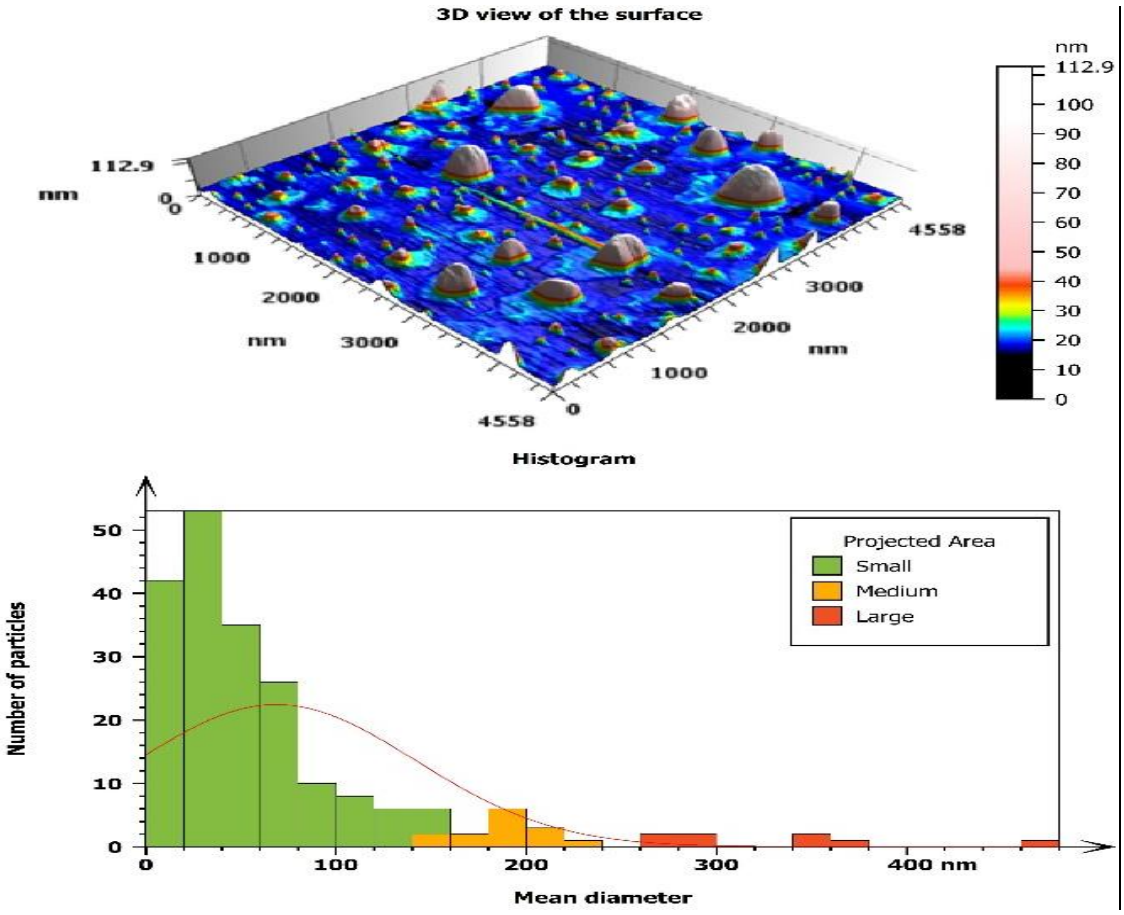

Fig. 3. The biosynthesized SeNPs under AFM 2D and 3D images of SeNPs.

Ethical Statement

This research was approved by the Committee of Ethical Standards in the College of Sciences / Baghdad University. The study protocol, subject information, and permission form were reviewed and approved by a local ethics committee the document number CSEC/1224/0127 dated December 25/2024.

Statistical Analysis

A one-way analysis of variance ANOVA (Tukey) and Student's t-test were performed to test whether group variance was significant or not. Statistical significance was defined as * $p < 0.05$ or ** $p < 0.01$. All samples analyzed statistically were run in triplicates. Data were expressed as mean ±standard deviation and statistical significances were carried out using GraphPad Prism version 9 (GraphPad Software Inc., La Jolla, CA).

RESULTS AND DISCUSSION

Synthesis of CS-SeNPs

The solution's color progressively changed from pale yellow to deep brownish orange after 30 minutes, signifying the greensynthesis of SeNPs.Visual and aural observation the color of the solution gradually changed from pale yellow to a deep brownish-orange tint after 60 minutes. Several metal NPs have been biosynthesised using PPE. Significant amounts of phenolic compounds, including hydrolyzable tannins and flavonoids, which are essential for the creation of metal nanoparticles, are present in pomegranate peel. PPE was used in the current investigation to manufacture SeNPs. The biogenesis of SeO NPs was then indicated by the weak red, white, and red hues that were seen, where PPE was serving as a capping or reducing agent. Bioactive phytochemicals included in plant extracts function as a capping agent, preventing the agglomeration of nanoparticles and altering their biological activity. The synthesis and capping of SeNPs using and biopolymers chitosan when added chitosan to selenium nanoparticles the color change to brown.

Characterization SeNPS

UV-Visible (UV-VIS) Spectroscopy

As seen an absorption peak in (Fig. 2a) of Se

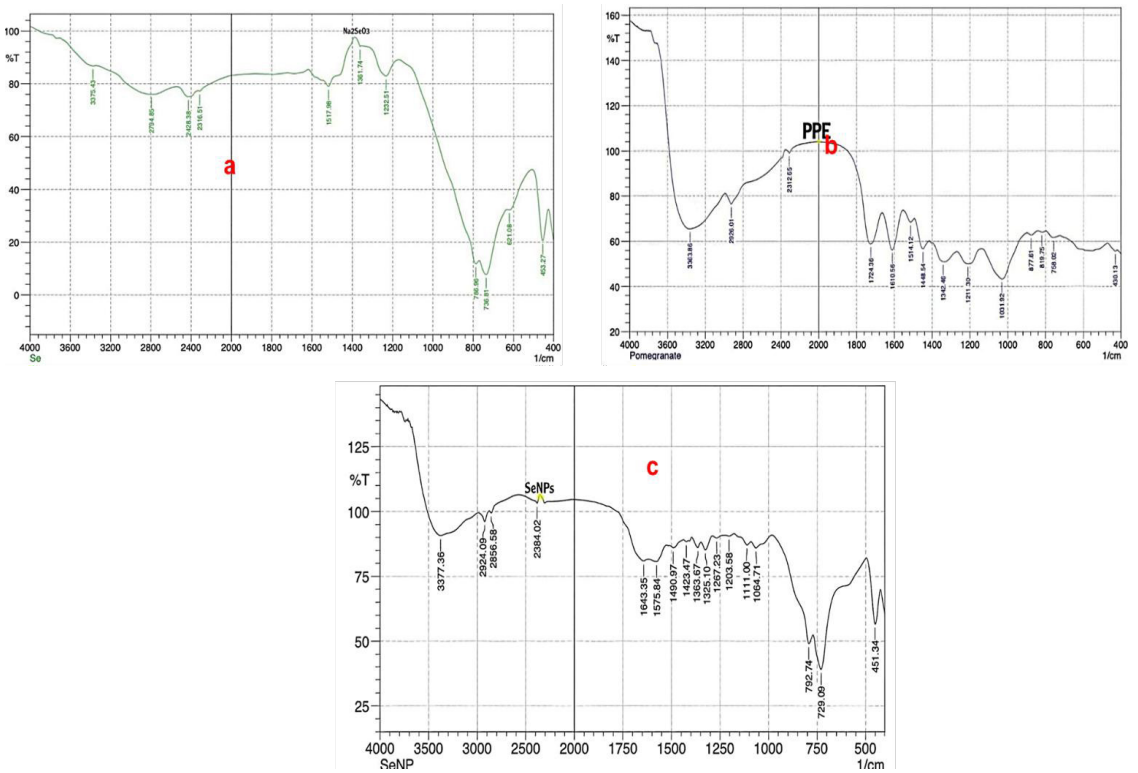

Fig .4. Infrared spectra of employed materials a) Na_2SeO_3 b) pomegranate peels (PPE) extract, (b)SeNPs (PPE/SeNPs)

at 217 nm of sodium selenite indicates successful PPE production can be seen (Fig. 2b) at the peak reached 362 nm. (Fig. 2c) illustrates the UV-visible 283nm method used to characterize the biosynthesized SeNPs, which included individual NPs. The UV-Vis spectra provided (Fig. 2 a–c) reveal critical insights into the synthesis of SeNPs using (PPE) as a green reducing agent. A sharp peak at 217 nm (or ~200–220 nm in some spectra) is characteristic of selenite ions (SeO_3^{2-}). This peak arises from $\pi \rightarrow \pi$ *electronic transitions* * in the Se=O bonds of the selenite ion. This confirms the presence of Na_2SeO_3 as the selenium precursor. The high absorbance at this wavelength indicates a concentrated solution of selenite ions. The notable peak at 362 nm (or ~360–370 nm) in the Na_2SeO_3 spectrum (Fig. 2b), suggests residual selenite ions or intermediates during nanoparticle synthesis. This peak is observed after PPE addition, it may indicate incomplete reduction of Se^{4+} to Se^{o}. Alternatively, the 362 nm peak could reflect impurities or side reactions during synthesis (e.g., partially reduced selenium species like SeO_2 or SeO_2^-).

Atomic force microscopy (AFM)

The average diameter of SeNPS, alongside their two- and three-dimensional shape, have been measured with atomic force microscopy as a confirming methodology for explaining their biogenesis in general. The study's result diameter, displayed in (Fig. 3), showed that the synthesized SeNPs exhibited a diameter of 68 nm.

FTIR analysis

The FT-IR spectra (Fig. 4a–c) provide critical insights into the chemical interactions between pomegranate peel extract (PPE), sodium selenite (Na_2SeO_3), and the resulting selenium nanoparticles (SeNPs). Below is a detailed breakdown of the spectral features and their implications for nanoparticle biosynthesis. The broad band at 3375 cm^{-1} attributed to O–H stretching vibrations. The sharp peak at 2428 cm^{-1}, corresponding to Se–O stretching vibrations in the SeO_3^{2-} ion, due to bending modes of H–O–H or H–O–Se groups at 1617 cm^{-1}, while the symmetric stretching of Se–O bonds at the 1361 cm^{-1}, and the deformation vibrations of Se–O–Se linkages at 1084 cm^{-1}. The spectrum at (Fig. 4a) reflects the inorganic nature of Na_2SeO_3, with dominant Se–O vibrations. The absence of organic functional groups confirms that Na_2SeO_3 serves purely as a selenium precursor. The PPE (Fig. 4b) spectrum at 3347 cm^{-1}

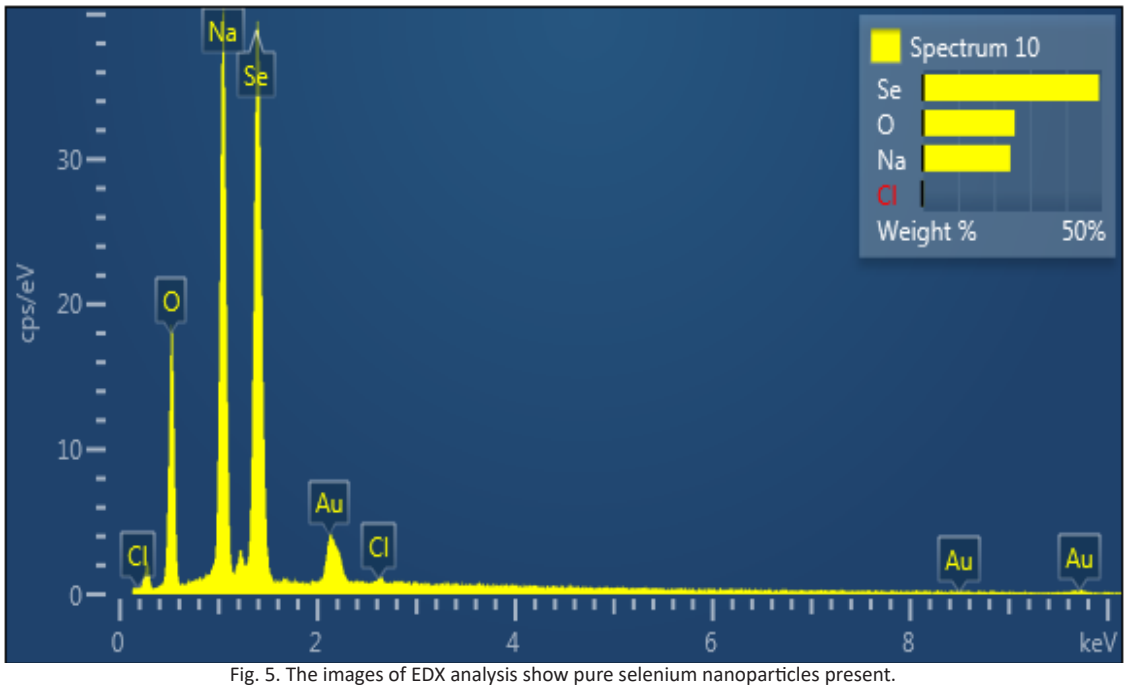

Fig. 5. The images of EDX analysis show pure selenium nanoparticles present.

is corresponding to strong O–H stretching (free or H-bonded hydroxyl groups in phenols, flavonoids, or tannins). The aliphatic C–H stretching at 2977 and 2888 cm^{-1} due to methylene/methyl groups in lipids or carbohydrates. The C=O stretching at 1723 cm^{-1} (carbonyl groups in esters, ketones, or amides). The aromatic C=C stretching at 1601 cm^{-1} (benzene rings in polyphenols like ellagic acid). The methylene (CH_2) deformation and symmetric stretching of $–COO^-$ groups at 1439 and 1361 cm^{-1}.

Energy dispersive X-ray (EDX)

The EDX analysis was used to determine the elemental composition of the SeNP powder. The existence of several different elements connected to the selenium, oxygen, sodium, and chloride components was shown by the EDX spectra of the SeNPs (Fig. 5).

Field emission Scanning Electron Microscope (FESEM)

The resulting Se-NPs had a uniform distribution and were spherical in shape, free of aggregations. The range of sizes between 10 and 60 nm was the primary average size of Se-NPs. TEM micrographs also demonstrated the homogeneous dispersion of the SeNPs. The SEM was used to evaluate the surface morphologies and particle sizes of SeNPs, as shown in (Fig .6). The shapes of SeNPs were nearly spherical.

X-ray diffraction method (XRD)

The predominant orientation occurred to plane (101) as seen by the greater and higher peak at 2h = 29.61 relating to the plane (101). The outcomes showed that the bio-synthesized Se-NPs were made of highly pure crystalline Se. Fig. 2S (Supplementary data) shows the Se-NPs' XRD pattern, which shows the produced Se-NPs' hexagonal structure. It is abundantly evident that the initial precursors lack any distinctive peaks. Bragg's reflections at (100), (101), (111), (201), and (210) are represented by the SeNPs XRD diffraction peaks and the diffraction characteristics

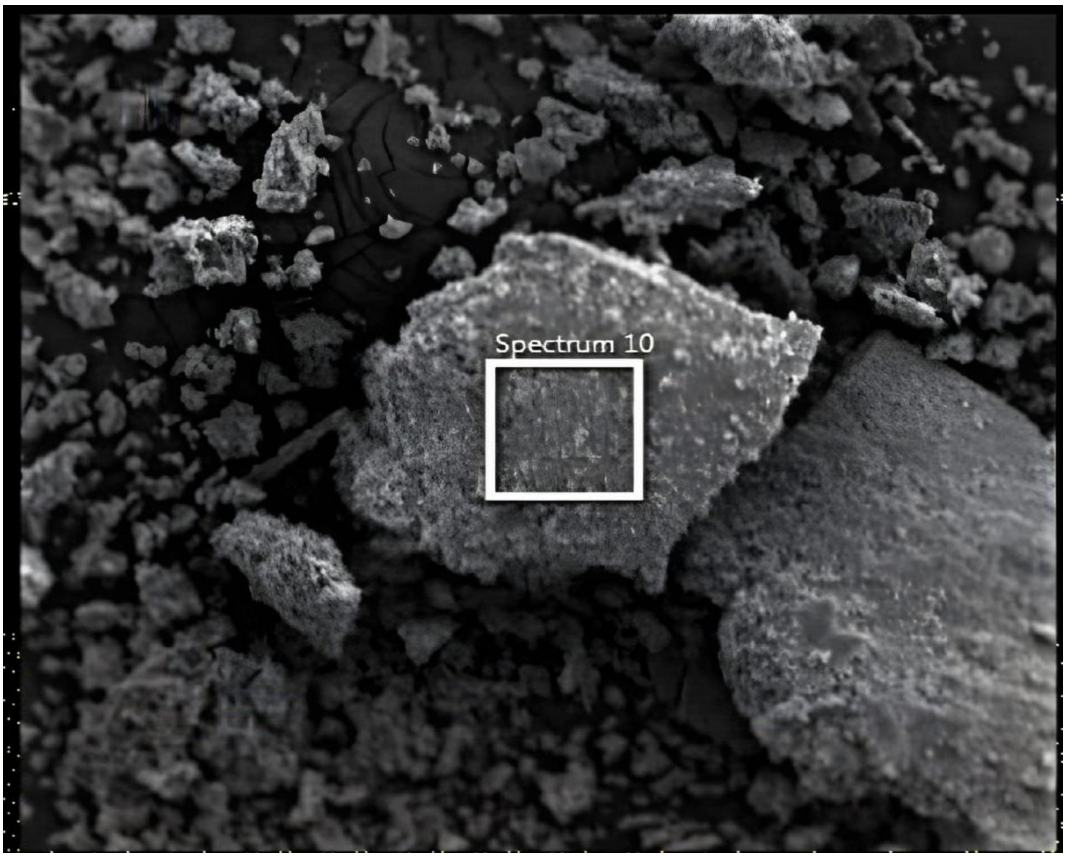

Fig. 6. SEM image, mapping of SeNPs prepared by PPE extract.

concerning 2θ at 23.46°, 30.08°, 41.76°, 53.12°, and 64.76°, respectively (Fig. 7). We explain the results by pointing out that previous studies have demonstrated that crystallite, cubic phase form SeNPs may be successfully fabricated at the same XRD diffraction planes using mediators derived from plant extracts, the generated SeNPs were extremely crystalline for improved application, according to the XRD data.

Antifungal activity of CS-SeNPs

The findings showed that both Se NPs and CS/SeNPs showed greater antifungal activity against all tested fungi, with an increase in inhibition that was concentration-dependent. Multiple explanations for chitosan's anti-fungal effects have been offered by scientists With the well diffusion method, the antifungal activity of the three produced nanostructures (CS/Se NPs and Se NPs) at doses (6.25–1000 µg/ml) was measured. For Candida glabrata, inhibition zones increased with concentration for both nanoparticles. At the lowest concentration (62.5 µg/mL), Se NPs exhibited an inhibition zone of 13.0 ± 1.0a mm, whereas CS/SeNPs showed a slightly higher inhibition of 11.3 ± 0.6a mm, however, from 125 µg/mL onwards, SeNPs demonstrated significantly greater antifungal activity compared to CS-SeNPs ($p < 0.01$). In the case of *Candida krusei*, -SeNPs displayed markedly higher antifungal efficacy than CS/SeNPs at concentrations above 62.5 µg/mL. At 125 µg/mL, Se NPs and CS-SeNPs showed inhibition zones of 11.3 ± 0.6a mm and 12.3 ± 0.6a mm, respectively, but the difference was not statistically significant ($p = 0.0006$). However, at 62.5 µg/mL and above, the difference became highly significant ($p < 0.0001$), with CS-SeNPs consistently producing larger inhibition zones. At the highest concentration (1000 µg/mL), Se NPs exhibited an inhibition zone of 26.7 ± 0.6e mm, whereas CS-Se NPs reached 16.3 ± 1.5c mm ($p < 0.0001$). At 62.5 µg/mL, the inhibition zone was 12.7 ± 0.6a mm for Se NPs and 12.0 ± 1.0a mm for CS-SeNPs, with no significant difference ($p = 0.5927$). However, at 125 µg/mL, the difference became significant ($p = 0.0027$), with inhibition zones of 17.3 ± 0.6b mm for Se NPs and 13.3 ± 1.2a mm for CS-Se NPs. At the highest concentration (1000 µg/mL), Se NPs produced an inhibition zone of 27.7 ± 0.6e mm, whereas CS-SeNPs showed a significantly higher inhibition zone of 18.7 ± 1.2b mm ($p < 0.0001$) (Fig. 8-b).

The cytotoxic effect of SeNP nanoparticles on tumor cell lines

The flow of materials like nutrients and oxygen to tumorous tissues is made possible by the vast vascular arteries and their pores The

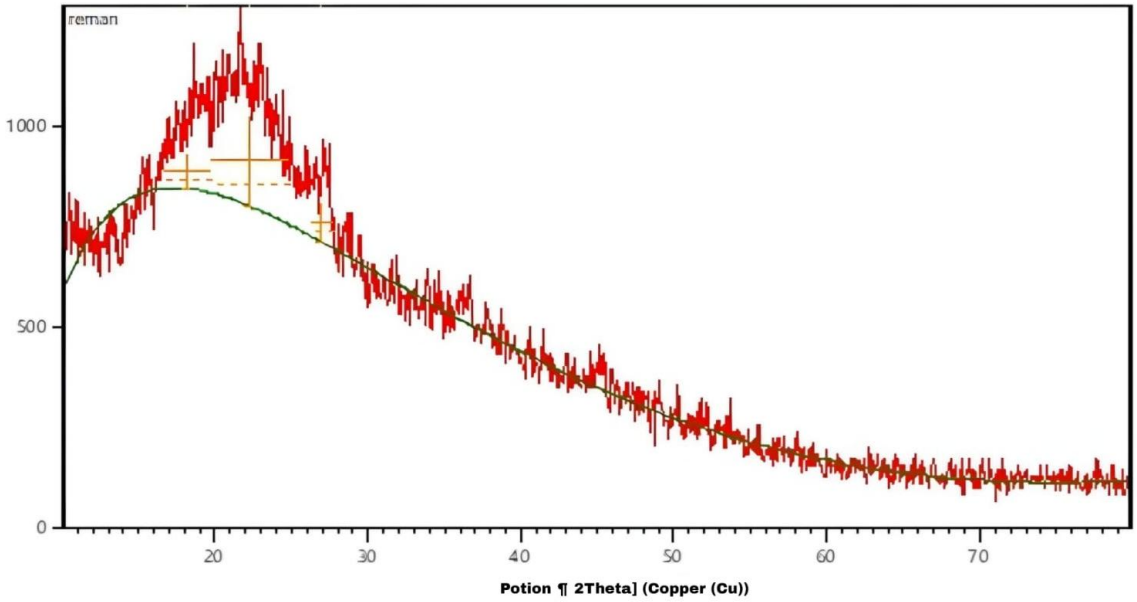

Fig. 7. Utilizing the XRD method to analyze the structural properties (SeNPs).

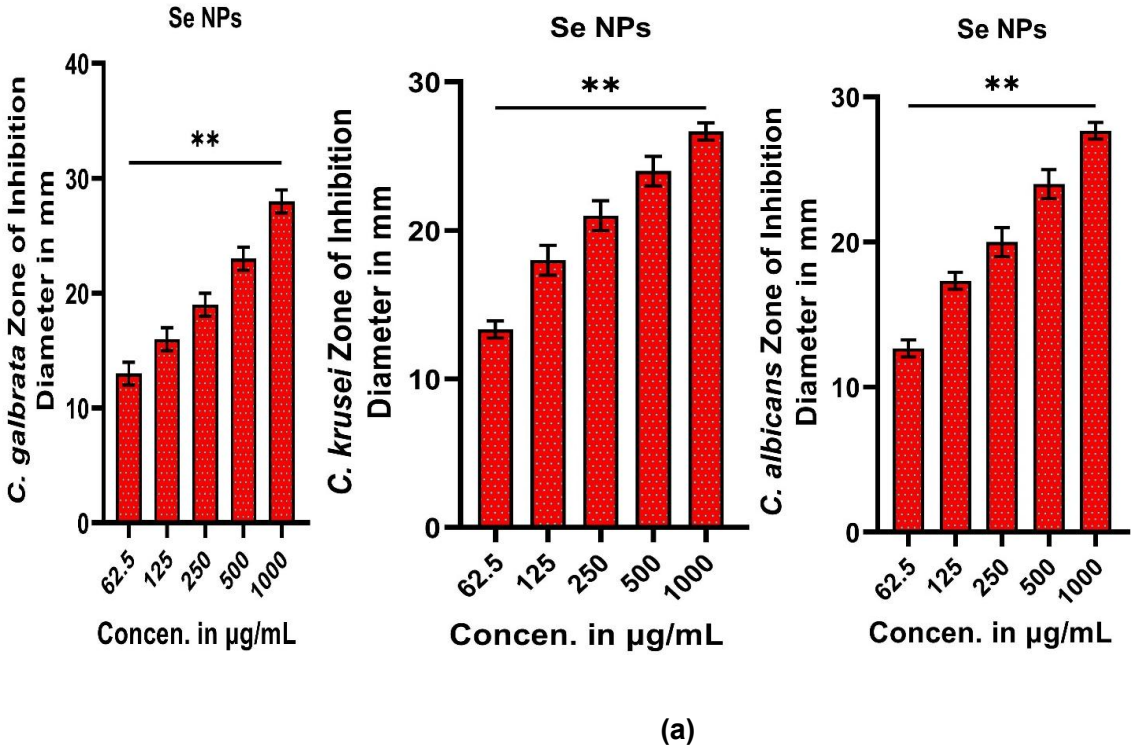

Fig. 8. Mean ± SD Zone of Inhibition in mm treated with a) SeNPs, b) CS-SeNPs against candida spp at Different Concentrations between 1000, 500, 250, 125, and 62.5µg/mL.: Standard Deviation, (n = 3).

first and most obvious change that occurs when cells are exposed to Se-NPs is a change in the morphological form of a monolayer culture. The cytotoxic activity of selenium nanoparticles on the human breast adenocarcinoma cell line MCF7 was studied as seen in (Fig. 9). Morphology of control cell and treatment cell with two concentrations (50 ug/ml and 100 ug/ml). Studies have indicated that as the concentration of SeNPs, cell viability declined. SeNPs had a GI 50 value of nearly 11 µg/ml· These NPs exhibited toxic effects against the MCF7 cell line, and at a concentration of 25 µg/ml, the cytotoxic effects reached 65.4%. SeNPs were tested for in vitro cytotoxicity against MCF7 cell lines at concentrations of 6.25–100 µg/ml illustrated in (Fig. 10).

Selenium nanoparticles (SeNPs) have emerged as promising candidates among various nanomaterials due to their notable biological activity, high bioavailability, and strong antioxidant properties. As a result, there has been growing interest in recent years in developing SeNP-based nanocomposite hydrogels for a wide range of biomedical applications [18]. These phytochemicals play a crucial role in the green synthesis of nanoparticles. For example, pomegranate peel extract (PPE) has been successfully used to synthesize gold and silver nanoparticles, referred to as PPE-MAuNPs and PPE-MAgNPs, respectively, supporting the broader category of PPE-mediated nanoparticles (PPE-MNPs) [19]. The color transition from pale yellow to deep brownish-orange during SeNP synthesis (Fig. 5) aligns with surface plasmon resonance (SPR) phenomena, a hallmark of nanoparticle formation. UV-Vis spectroscopy revealed a characteristic peak at 283 nm, attributed to polyphenolic compounds in PPE (e.g., ellagic acid, punicalagin), confirming their dual role as reducing and capping agents. This is consistent with prior studies where plant-derived polyphenols mediated nanoparticle synthesis via redox reactions]. The FTIR spectrum of the synthesized SeNPs revealed notable shifts in the O–H and N–H stretching vibrations, suggesting strong interactions between the pomegranate peel extract (PPE) metabolites and the nanoparticle surface. These interactions are believed to contribute to the stabilization of the nanoparticles by preventing aggregation and enhancing their biocompatibility. A distinct peak observed at 1631 cm^{-1}, which shifted to 1644 cm^{-1}, indicates the formation of Se–O bonds. Additionally, a band appearing at 879 cm^{-1} was attributed to Se–O stretching vibrations, further confirming the successful formation and surface functionalization of the selenium nanoparticles [20]. The sizes and forms of the generated chitosan nanoparticles and their nanocomposites were investigated. Semispherical in shape, the particles had an interconnected structure, some aggregation, and an average size of 30 to 40 nm. An ionic interaction between the positively charged amino groups of chitosan (protonated amines in aqueous acetic acid solution) and the negatively charged sodium tripolyphosphate produced these semi-spherical nanoparticles. LC50 values for the plant-mediated production of Se-NPs against Anopheles stephensi, Aedes aegypti, and Culex quinquefasciatus larvae were found to be higher at 240.714 ppm, 104.13 ppm, and 99.602 ppm, respectively [21]. The phytocompounds present in the plant extract likely play a critical role in the biosynthesis and stabilization of selenium nanoparticles (SeNPs). Its microbicidal activity is largely attributed to its positively charged surface, which facilitates strong electrostatic interactions with negatively charged microbial cell membranes. This interaction disrupts membrane integrity, increases permeability, and interferes with intracellular components. Moreover, chitosan is known to enhance reactive oxygen species (ROS) generation and inhibit vital cellular functions, thereby amplifying its antimicrobial effects [22]. These results suggest that each component retained its bioactivity while contributing to an enhanced collective effect. The incorporation of nanometals such as SeNPs is known to amplify the overall efficacy of such composites, enhancing their antioxidant, antimicrobial, and even anticancer properties through synergistic interactions at the nanoscale [23]. It is proposed that this novel nanocomposite (NCT/PPE/SeNPs) has several functions. Firstly, the NCT transports/holds PPE/SeNPs to the fungal hypha and attaches/interacts with them to soften and partially lyse membranes; second, it may enter the hypha and the released PPE/SeNPs can interact with intracellular organelles/biosystems to inhibit their essential functions, which in turn causes fungal deformation and lysis.CS, a polysaccharide derivative of chitin that is taken from fungi and arthropods like crustaceans and insects, was another substance that was evaluated in this study either alone or in combination with SeNPs. It effectively caps and stabilizes SeNPs and

has fungicidal properties. This polymer is naturally occurring, biocompatible, biodegradable, bioadhesive, positively charged, and has minimal cytotoxicity. It is well known that CS has fungicidal and microbicidal effects. We draw the conclusion that CS-SeNPs work in concert to effectively inhibit the premade cell in vitro through dose-response inhibition. To fully comprehend the synergistic action of Se and CS together against Candida spp., more research is necessary. The MTT assay revealed dose-dependent cytotoxicity of SeNPs against MCF7 breast cancer cells, with a GI_{50} of 11 µg/mL (Fig. 10). Although the cytotoxicity of CS-SeNPs was not explicitly quantified in this study, chitosan's established role as a drug delivery vehicle suggests its potential to enhance targeted uptake by cancer cells while minimizing off-target effects. The effectiveness of such nanocomposites is closely linked to key physicochemical properties—particularly nanoparticle size and surface

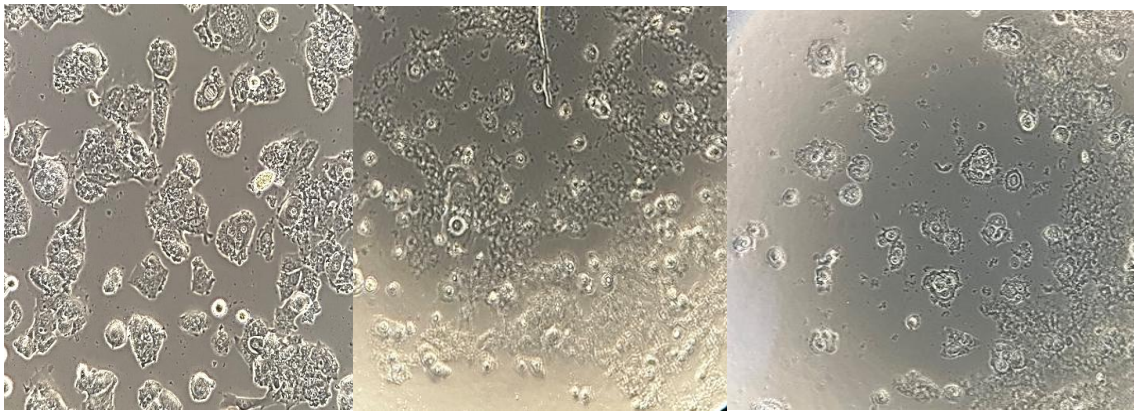

Fig. 9. The cytotoxic effect of SeNPs a) Control MCF7 cells, at concentration b) 50 ug/ml c) 100 ug/ml.

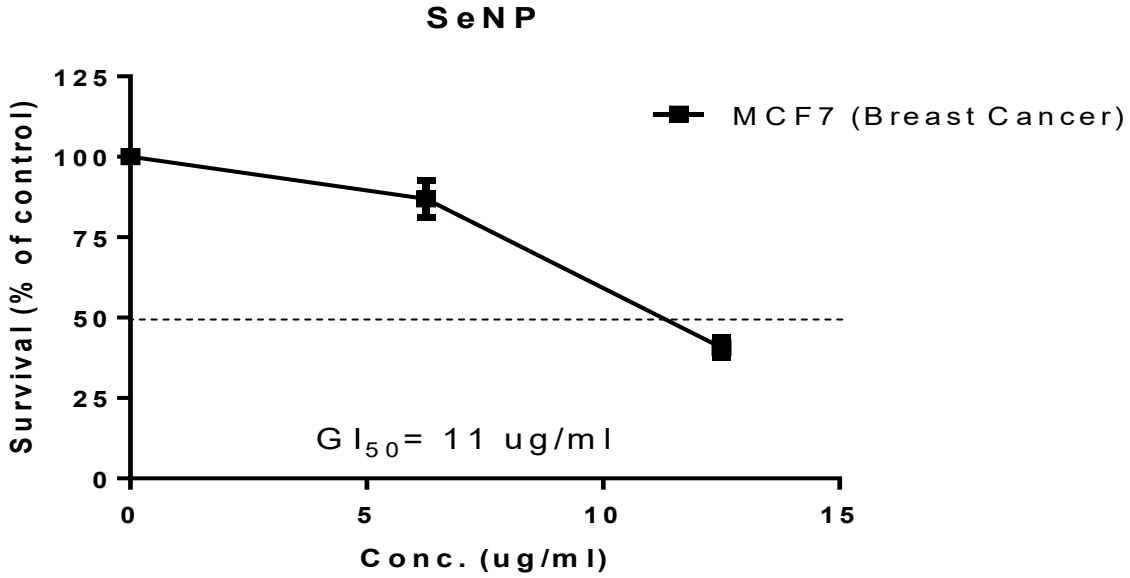

Fig .10. The cytotoxic effect of SeNPs on MCF7 cells.

charge—which govern cellular internalization and biodistribution. The SeNPs synthesized in this study showed an average size of 68 nm by AFM, placing them within the optimal range for cellular uptake via endocytosis (<100 nm). However, these coatings may influence colloidal stability, circulation time, and interactions with biological membranes, all of which are critical factors for biomedical applications such as targeted cancer therapy [24]. The study aimed to evaluate the antifungal efficacy of the resulting nanocomposite against *Candida* species and assess its cytotoxic effects on human breast cancer (MCF-7) cells, with a focus on exploring its potential for biomedical applications.

CONCLUSION

Because it is environmentally friendly and biocompatible, the biosynthesis of Se-NPs using microorganisms is a new trend in bio-nanotechnology that has several uses in the biomedical arena. The field of biogenic synthesis of nanoparticles utilizing plant extracts or microbes has gained more attention in the past few decades. The green approach has gained greater attention because it is safe, non-toxic, accessible, and affordable. The nanoparticles are more efficient at catalyzing the breakdown of dyes found in wastewater from a variety of industries due to their high surface-to-volume ratio and tuneable surface plasmon resonance. Selenium nanoparticles have special qualities among the several kinds of nanoparticles used ther medicinal applications. Furthermore, Se nanoparticles exhibit superior biodegradability and biocompatibility When tested against the non-tumor cell line all produced composite nanoparticles showed extremely minimal cytotoxicity. The produced CS-Se-NPs nanocomposite provided a high-efficiency, low-cost system that may be suggested as a promising cancer treatment vehicle.

CONFLICT OF INTEREST

The authors declare that there is no conflict of interests regarding the publication of this manuscript.

REFERENCES

1. Danish MSS, Estrella-Pajulas LL, Alemaida IM, Grilli ML, Mikhaylov A, Senjyu T. Green Synthesis of Silver Oxide Nanoparticles for Photocatalytic Environmental Remediation and Biomedical Applications. Metals. 2022;12(5):769.
2. Selvaraj B, A KK, S K, G S. Biogenic synthesis of selenium nanoparticles by moderate halophilic bacteria and evaluation of its anti-bacterial and anti-biofilm activity. Springer Science and Business Media LLC; 2023.
3. Ahmed Mais E, Sulaiman Ghassan M, Hasoon Buthenia A, Khan Riaz A, Mohammed Hamdoon A. Green Synthesis and Characterization of Apple Peel-Derived Selenium Nanoparticles for Anti-Fungal Activity and Effects of MexA Gene Expression on Efflux Pumps in Acinetobacter baumannii. Appl Organomet Chem. 2024;39(2).
4. Fawzi FH, Ahmed ME. Green Synthesis and Characterization of Selenium Nanoparticles via Staphylococcus warneri Approach: Antimicrobial and on PhzM Pyocyanin Gene Expression in Pseudomonas aeruginosa. Plasmonics. 2024.
5. Banerjee M, Rajeswari D. Green synthesis and anti-biofilm effect on Drosophila melanogaster of selenium nanoparticles from Vitis vinifera for photocatalytic degradation and different biological applications. Vietnam Journal of Chemistry. 2024;63(1):81-100.
6. Azmat F, Safdar M, Ahmad H, Khan MRJ, Abid J, Naseer MS, et al. Phytochemical profile, nutritional composition of pomegranate peel and peel extract as a potential source of nutraceutical: A comprehensive review. Food Science & Nutrition. 2024;12(2):661-674.
7. Panza O, Conte A, Del Nobile MA. Pomegranate By-Products as Natural Preservative to Prolong the Shelf Life of Breaded Cod Stick. Molecules. 2021;26(8):2385.
8. Mahmood RI, Al-Taie A, Al-Rahim AM, Mohammed-Salih HS, Ibrahim HA, Albukhaty S, et al. Biogenic synthesized selenium nanoparticles combined chitosan nanoparticles controlled lung cancer growth via ROS generation and mitochondrial damage pathway. Nanotechnology Reviews. 2025;14(1).
9. Habeeb ZA, Jameel SK, Ahmed ME. Synthesis, Characterization, and Cytotoxic Evaluation of Selenium Nanoparticles. Biomedical and Pharmacology Journal. 2025;18(1):909-919.
10. Salem MF, Abd-Elraoof WA, Tayel AA, Alzuaibr FM, Abonama OM. Antifungal application of biosynthesized selenium nanoparticles with pomegranate peels and nanochitosan as edible coatings for citrus green mold protection. Journal of Nanobiotechnology. 2022;20(1).
11. Menon S, Agarwal H, Rajeshkumar S, Jacquline Rosy P, Shanmugam VK. Investigating the Antimicrobial Activities of the Biosynthesized Selenium Nanoparticles and Its Statistical Analysis. BioNanoScience. 2020;10(1):122-135.
12. Alghuthaymi MA, Diab AM, Elzahy AF, Mazrou KE, Tayel AA, Moussa SH. Green Biosynthesized Selenium Nanoparticles by Cinnamon Extract and Their Antimicrobial Activity and Application as Edible Coatings with Nano-Chitosan. J Food Qual. 2021;2021:1-10.
13. Salman MF, Al-Mudallal NHAL, Ahmed ME. Cytotoxic Effect of Biogenic Selenium Nanoparticles Using Bacteriocin of Acinetobacter baumannii Isolated from Burns and Wound Infections. Iraqi Journal of Science. 2025:1535-1549.
14. Shehab ZH, Ahmed ST, Abdallah NM. Genetic variation of pilB gene in Pseudomonas aeruginosa isolated from Iraqi patients with burn infections. Annals of Tropical Medicine and Public Health. 2020;23(16).
15. Hosseini Bafghi M, Zarrinfar H, Darroudi M, Zargar M, Nazari R. Green synthesis of selenium nanoparticles and evaluate their effect on the expression of ERG3, ERG11 and FKS1 antifungal resistance genes in Candida albicans and

Candida glabrata. Lett Appl Microbiol. 2022;74(5):809-819.
16. Ahmed ME, Alzahrani KK, Fahmy NM, Almutairi HH, Almansour ZH, Alam MW. Colistin-Conjugated Selenium Nanoparticles: A Dual-Action Strategy Against Drug-Resistant Infections and Cancer. Pharmaceutics. 2025;17(5):556.
17. Faiq NH, Ahmed ME. Effect of Biosynthesized Zinc oxide Nanoparticles on Phenotypic and Genotypic Biofilm Formation of Proteus mirabilis. Baghdad Science Journal. 2024;21(3):0894.
18. Golmohammadi R, Najar-Peerayeh S, Tohidi Moghadam T, Hosseini SMJ. Synergistic Antibacterial Activity and Wound Healing Properties of Selenium-Chitosan-Mupirocin Nanohybrid System: An in Vivo Study on Rat Diabetic Staphylococcus aureus Wound Infection Model. Scientific Reports. 2020;10(1).
19. Tsekhmistrenko Sc, Bityutskyy V, Tsekhmistrenko O, Merzlo S, Tymoshok N, Melnichenko A, et al. Bionanotechnologies: Synthesis of Metals' Nanoparticles with Using Plants and Their Applications in the Food Industry: A Review. Journal of microbiology, biotechnology and food sciences. 2021;10(6):e1513.
20. Abdelhamid AE, Ahmed EH, Awad HM, Ayoub MMH. Synthesis and cytotoxic activities of selenium nanoparticles incorporated nano-chitosan. Polym Bull. 2023;81(2):1421-1437.
21. Jaafar FN, Salman HA, Ali SM, Ahmed ZM. Incidence of resistance pattern and biofilm-forming genes of Acinetobacter baumannii isolated from Iraqi children. Microbes and Infectious Diseases. 2025;0(0):0-0.
22. Ganachari SV, Yaradoddi JS, Somappa SB, Mogre P, Tapaskar RP, Salimath B, et al. Green Nanotechnology for Biomedical, Food, and Agricultural Applications. Handbook of Ecomaterials: Springer International Publishing; 2019. p. 2681-2698.
23. Faiq NH, Ahmed ME. Inhibitory Effects of Biosynthesized Copper Nanoparticles on Biofilm Formation of Proteus mirabilis. Iraqi Journal of Science. 2024:65-78.
24. Hamed AA, Hawwa MT, Baraka DM, El-Shora HM, El-Sayyad GS, Al-Hazmi NE, et al. Understanding antimicrobial activity of biogenic selenium nanoparticles and selenium/chitosan nano-incorporates via studying their inhibition activity against key metabolic enzymes. Int J Biol Macromol. 2025;298:140073.